Nucleocytoplasmic shuttling of persistently activated STAT3

Andreas Herrmann[1,*,‡], Michael Vogt[1,*], Martin Mönnigmann[2,§], Thomas Clahsen[1], Ulrike Sommer[1], Serge Haan[1], Valeria Poli[3], Peter C. Heinrich[1] and Gerhard Müller-Newen[1,¶]

[1]Institut für Biochemie, Universitätsklinikum RWTH Aachen, Pauwelsstraße 30, 52074 Aachen, Germany
[2]Lehrstuhl für Prozesstechnik, RWTH Aachen, Templergraben 55, 52056 Aachen, Germany
[3]Department of Genetics, Biology and Biochemistry, Molecular Biotechnology Center, University of Turin, Via Nizza 52, 10126 Torino, Italy

*These authors contributed equally to this work
‡Present address: Division of Cancer Immunotherapeutics and Tumor Immunology, Beckman Research Institute at the City of Hope National Medical Center, Duarte, CA 91010, USA
§Present address: Technische Universität Braunschweig, 38023 Braunschweig, Germany
¶Author for correspondence (e-mail: mueller-newen@rwth-aachen.de)

Accepted 5 July 2007
Journal of Cell Science 120, 3249-3261 Published by The Company of Biologists 2007
doi:10.1242/jcs.03482

Summary

Persistent activation of the transcription factor STAT3 has been detected in many types of cancer and plays an important role in tumor progression, immune evasion and metastasis. To analyze persistent STAT3 activation we coexpressed STAT3 with v-Src. We found that tyrosine phosphorylation of STAT3 by v-Src is independent of Janus kinases (Jaks), the canonical activators of STATs. The STAT3-induced feedback inhibitor, suppressor of cytokine signaling 3 (SOCS3), did not interfere with STAT3 activation by v-Src. However, the protein inhibitor of activated STAT3 (PIAS3) suppressed gene induction by persistently activated STAT3. We measured nucleocytoplasmic shuttling of STAT3 in single cells by bleaching the YFP moiety of double-labelled STAT3-CFP-YFP in the cytoplasm. Analysis of the subcellular distribution of CFP and YFP fluorescence over time by mathematical modeling and computational parameter estimation revealed that activated STAT3 shuttles more rapidly than non-activated STAT3. Inhibition of exportin-1-mediated nuclear export slowed down nucleocytoplasmic shuttling of v-Src-activated STAT3 resulting in reduced tyrosine phosphorylation, decreased induction of STAT3 target genes and increased apoptosis. We propose passage of persistently activated STAT3 through the nuclear pore complex as a new target for intervention in cancer.

Supplementary material available online at
http://jcs.biologists.org/cgi/content/full/120/18/3249/DC1

Key words: STAT3, v-Src, iFLAP, Nucleocytoplasmic shuttling, Apoptosis, Cancer

Introduction

The transcription factor STAT3 has multiple functions in fertility, embryonal development, the acute-phase response of the liver and the regulation of immune responses (Levy and Lee, 2002). Only recently, the importance of dysregulated STAT3 activation for the progression of cancer has been fully recognized (Darnell, 2005; Yu and Jove, 2004). STAT3 not only acts cell-autonomously by stimulating cell proliferation and preventing apoptosis but also facilitates immune evasion of tumor cells (Wang et al., 2004). STAT3 promotes tumor angiogenesis through the induction of VEGF (Niu et al., 2002) and by acting downstream of the VEGF receptor (Yahata et al., 2003). Furthermore, a function of STAT3 in tumor invasion and metastasis by upregulation of matrix metalloproteinases has been established (Itoh et al., 2005). STAT3 consists of an N-terminal multimerization domain, followed by a coiled-coil domain, the DNA-binding domain, a single SH2 domain and finally the transactivation domain (TAD). The tyrosine residue Y705 of STAT3 phosphorylated upon activation is located between the SH2-domain and the TAD and mediates STAT3 dimerization through reciprocal phosphotyrosine/SH2-domain interactions (Levy and Lee, 2002).

The family of IL-6-type cytokines that signal through the cytokine receptor gp130 are the most potent physiological activators of STAT3 (Heinrich et al., 2003). Upon ligand binding, STAT3 is phosphorylated at Y705 by receptor-associated Jak1. Activated STAT3 dimers accumulate in the nucleus, where they induce target genes (Lütticken et al., 1994; Stahl et al., 1994). Among other proteins, the feedback inhibitor SOCS3 is induced by STAT3. SOCS3 inhibits Jak1 at the receptor leading to attenuation of Jak1/STAT3 signalling (Nicholson et al., 2000; Schmitz et al., 2000). Besides cytokines, some growth factors such as EGF and PDGF activate STAT3. Activation of STAT3 by receptor tyrosine kinases has been reported to be mediated by Src-dependent and Src-independent mechanisms (Olayioye et al., 1999; Sachsenmaier et al., 1999; Wang et al., 2000).

Although constitutive activation of STAT3 has been observed in an increasing number of cancer types, not a single case of a naturally occuring oncogenic mutation within the STAT3 gene has been reported. Rather, STAT3 is activated by dysregulated upstream signalling pathways including cytokine and growth factor receptor signalling and other oncogenic tyrosine kinases such as Src family kinases or Alk kinase (Yu and Jove, 2004). v-Src has been identified to be a strong activator of STAT3 (Cao et al., 1996; Yu et al., 1995). Most

importantly, constitutive activation of STAT3 is required for transformation of cells by v-Src (Bromberg et al., 1998; Schlessinger and Levy, 2005).

Cytokine-induced STAT3 phosphorylation is transient, peaking within 30 minutes after stimulation and declining within the following 30 minutes, whereas in v-Src-transformed cells STAT3 is persistently phosphorylated. Thus, activation of STAT3 by v-Src seems to be less sensitive to the various inhibitors of Jak/STAT signalling such as SOCS feedback inhibitors, SUMO ligases of the PIAS family or the tyrosine phosphatases involved in dephosphorylation of Jaks and STATs. Indeed, STAT3-activation by v-Src is not disturbed by overexpression of SOCS1 (Iwamoto et al., 2000). In this respect, the STAT3-relevant inhibitors SOCS3 and PIAS3 have not been analyzed.

Even less is known about the intracellular dynamics of constitutive STAT3 activation by v-Src. Owing to the membrane-anchorage of v-Src (Sefton et al., 1982), phosphorylation of STAT3 is expected to occur exclusively at the cytoplasmic leaflet of membranes. Phosphorylated STAT3 is rapidly dephosphorylated within the nucleus (ten Hoeve et al., 2002). Therefore, in the presence of active nuclear phosphatases, persistent activation of STAT3 requires a continuous cycle of phosphorylation in the cytoplasmic compartment after dephosphorylation within the nucleus.

Recently, we analyzed the nucleocytoplasmic shuttling of STAT3 in unstimulated cells by iFLAP (intramolecular fluorescence localization after photobleaching) (Pranada et al., 2004). For this purpose we double-labelled STAT3 with cyan fluorescent protein (CFP) and yellow fluorescent protein (YFP). In the resulting fusion protein STAT3-CFP-YFP (STAT3-CY) the YFP moiety can be selectively bleached by the 514 nm laser of a confocal microscope. By bleaching YFP in the cytoplasm and detecting a decrease in the ratio of YFP to CFP fluorescence in the nucleus, we firmly established a constitutive nucleocytoplasmic shuttling of STAT3 in unstimulated cells that is independent of tyrosine phosphorylation (Pranada et al., 2004).

In the present study we set out to investigate the persistent activation of STAT3 by v-Src and to analyze the nucleocytoplasmic shuttling of activated STAT3 in single cells in real time. We found that activation of STAT3 by v-Src does not require Jaks and is insensitive to SOCS3. Using the above described iFLAP approach combined with quantitative evaluation of the data by mathematical modelling we found that STAT3 persistently activated by v-Src shuttles more rapidly between the cytoplasm and the nucleus than non-activated STAT3. Inhibition of the STAT3 reactivation cycle by blockade of nuclear export leads to reduced STAT3 phosphorylation, decreased induction of STAT3-responsive genes and apoptosis of v-Src-transformed fibroblasts. From our results, we propose that the transit of STAT3 through the nuclear pore complex is a promising target for the treatment of various malignancies.

Results

Activation of fluorescently labelled STAT3 by v-Src

In order to prove that fluorescently labelled STAT3 is a target for tyrosine phosphorylation by v-Src we co-transfected COS-7 cells with v-Src and STAT3, STAT3-YFP or various STAT3-YFP mutants and detected tyrosine phosphorylation of STAT3 by western blotting. As shown in Fig. 1, in the presence of v-Src or in response to IL-6 stimulation, STAT3-YFP is tyrosine phosphorylated (Fig. 1B, lanes 1-4) as is non-tagged STAT3 (Fig. 1A). A STAT3-YFP deletion mutant that lacks the N-terminal domain and the coiled-coil domain of STAT3 but retains the SH2-domain and tyrosine 705 [STAT3(321-771)-YFP] is neither a substrate for phosphorylation by v-Src nor by IL-6 (Fig. 1B, lanes 5-8). The lack of tyrosine phosphorylation of an SH2 domain-defective STAT3(R609Q)-YFP mutant indicates that phosphorylation of STAT3 by both IL-6 and v-Src requires a functional SH2-domain. As expected, no tyrosine phosphorylation of the mutant STAT3(Y705F)-YFP is detectable beyond background level (Fig. 1B, lanes 9-16).

In order to analyze fluorescent STAT3 fusion proteins in more detail we stably transfected murine embryonic fibroblasts lacking endogenous STAT3 ($MEF^{\Delta/\Delta}$) with STAT3-YFP ($MEF^{\Delta/\Delta}$STAT3-YFP) or STAT3-CY ($MEF^{\Delta/\Delta}$STAT3-CY). DNA binding in response to IL-6/sIL-6Rα stimulation was analyzed by EMSA (Fig. 1C). In MEF cells with the STAT3 alleles flanked by loxP sites ($MEF^{fl/fl}$) stimulation leads to the expected DNA-binding of STAT3/3 and STAT1/1 homodimers as well as STAT3/1 heterodimers. In cells lacking STAT3, STAT1 is predominantly activated (Costa-Pereira et al., 2002). In $MEF^{\Delta/\Delta}$STAT3-YFP cells a prominent band is observed upon stimulation that could be identified as STAT3-YFP by supershift with both STAT3 and GFP antibodies (Fig. 1C). Thus, upon activation, fluorescently labelled STAT3 binds to its DNA target sequence.

We analyzed the subcellular distribution of fluorescently labelled STAT3 by confocal laser-scanning microscopy and tyrosine phosphorylation by western blotting. In $MEF^{\Delta/\Delta}$STAT3-YFP cells co-transfected with v-Src, STAT3-YFP is predominantly located in the nucleus and tyrosine phosphorylated (Fig. 1D). Similarly, in $MEF^{\Delta/\Delta}$STAT3-CY cells co-transfected with v-Src, STAT3-CY accumulates in the nucleus and tyrosine phosphorylation is detectable in the western blot (Fig. 1E). As previously observed in IL-6-stimulated cells (Herrmann et al., 2004) (Fig. 2A), activated STAT3 accumulates in nuclear bodies in a subpopulation of cells. Mutants of STAT3-YFP that are not phosphorylated on tyrosine-705 do not accumulate in the nucleus, neither in v-Src-transfected cells nor in response to IL-6 stimulation (not shown). Activation of STAT3 by v-Src is quite specific since co-transfection of the kinases Fyn, Abl or BCR-Abl into MEF cells did not result in prominent phosphorylation of endogenous STAT3 or transfected STAT3-YFP (Fig. 1F). The STAT3 loading control in the western blot (Fig. 1F) shows that overexpression of STAT-YFP in $MEF^{\Delta/\Delta}$STAT3-YFP cells is moderate compared with endogenous STAT3 levels in $MEF^{fl/fl}$ cells.

Activation of STAT3 by v-Src is independent of Jak1, insensitive to SOCS3 but sensitive to PIAS3

The fact that STAT3 mutants that do not respond to IL-6 stimulation are not phosphorylated by v-Src suggests that activation of STAT3 by IL-6 and v-Src shares a common mechanism. Since a contribution by Jak1 in the phosphorylation of STAT3 by v-Src has been reported (Zhang et al., 2000b), we investigated whether Jaks are required for the activation of STAT3-YFP by v-Src. In parental 2C4

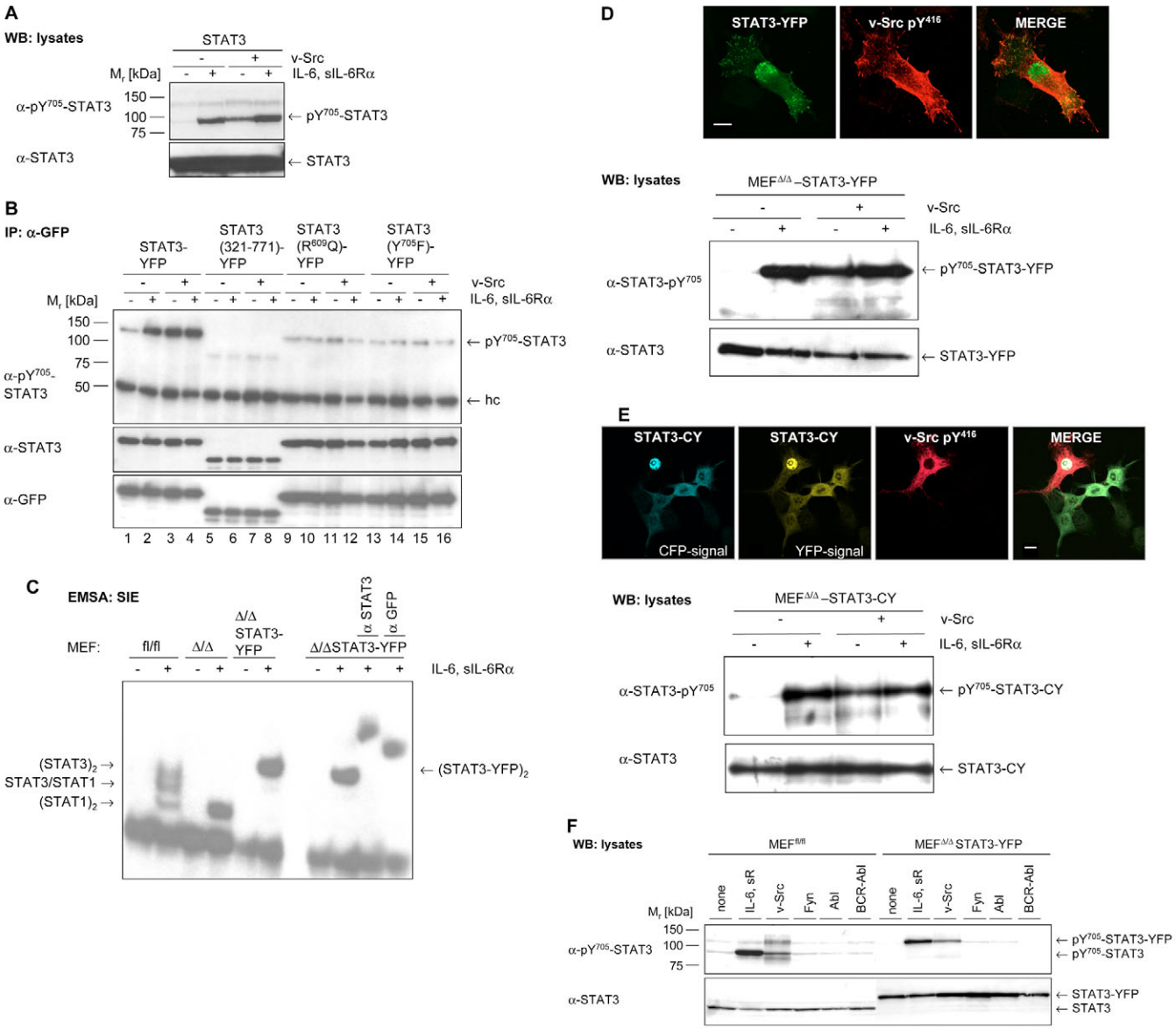

Fig. 1. v-Src expression leads to constitutive activation of wild-type and fluorescent STAT3 fusion proteins. (A) COS-7 cells were transiently transfected with v-Src and STAT3 as indicated and stimulated with 20 ng/ml IL-6 and 1 μg/ml sIL-6Rα for 30 minutes or left untreated. Whole cell lysates were subjected to SDS-PAGE and western blotting. STAT3 tyrosine phosphorylation was detected with a pY^{705}-STAT3 antibody and as a loading control STAT3 was counterstained with a specific STAT3 antibody. (B) Transiently expressed STAT3-YFP and mutant fusion proteins as indicated were precipitated from COS-7 cell lysates with a GFP antibody that recognizes YFP and CFP. Western blot analyses of precipitates were performed for pY^{705}-STAT3 and counterstained for total STAT3 and YFP. hc, heavy chain of the precipitating antibody. (C) Nuclear extracts were prepared from $MEF^{fl/fl}$, $MEF^{\Delta/\Delta}$ or $MEF^{\Delta/\Delta}$STAT3-YFP cells stimulated with 20 ng/ml IL-6 and 1 μg/ml sIL-6Rα for 30 minutes as indicated. STAT3, STAT1 and STAT3-YFP DNA-binding to a [^{32}P]-labelled SIE-probe was detected by EMSA. Antibodies against STAT3 and GFP were used for the supershift experiment. (D) $MEF^{\Delta/\Delta}$STAT3-YFP cells were co-transfected with v-Src, fixed and stained for pY^{416}-Src. Fixed cells were analyzed by confocal laser-scanning microscopy. Bars, 10 μm. A Western blot of lysates of $MEF^{\Delta/\Delta}$STAT3-YFP cells was analyzed for pY^{705}-STAT3 and counter-stained for total STAT3. (E) $MEF^{\Delta/\Delta}$STAT3-CY cells were treated and analyzed as described in D. Bars, 10 μm. A Western blot of lysates of $MEF^{\Delta/\Delta}$STAT3-CY cells was analyzed for pY^{705}-STAT3 and counter-stained for total STAT3. (F) $MEF^{fl/fl}$ and $MEF^{\Delta/\Delta}$STAT3-YFP cells were transfected with v-Src, Fyn, Abl, or BCR-Abl or left untransfected for IL-6 stimulation and the negative control as indicated. Whole cell lysates were subjected to western blotting and analyzed for pY^{705}-STAT3 and total STAT3 as a loading control.

fibrosarcoma cells, stimulation with IL-6/sIL-6Rα as well as co-transfection of v-Src leads to nuclear translocation of STAT3-YFP (Fig. 2A, left panel). In Jak1-deficient U4C fibrosarcoma cells, stimulation with IL-6/sIL-6Rα does not activate STAT3-YFP, whereas co-transfection with v-Src still leads to nuclear accumulation of STAT3-YFP (Fig. 2A, right panel). Similarly, STAT3-YFP is activated by v-Src in γ2A-cells and U1A-cells lacking Jak2 and Tyk2, respectively (data not shown). Treatment of v-Src-transfected HepG2 cells with the Jak inhibitor 1 that inhibits all Jaks does not influence

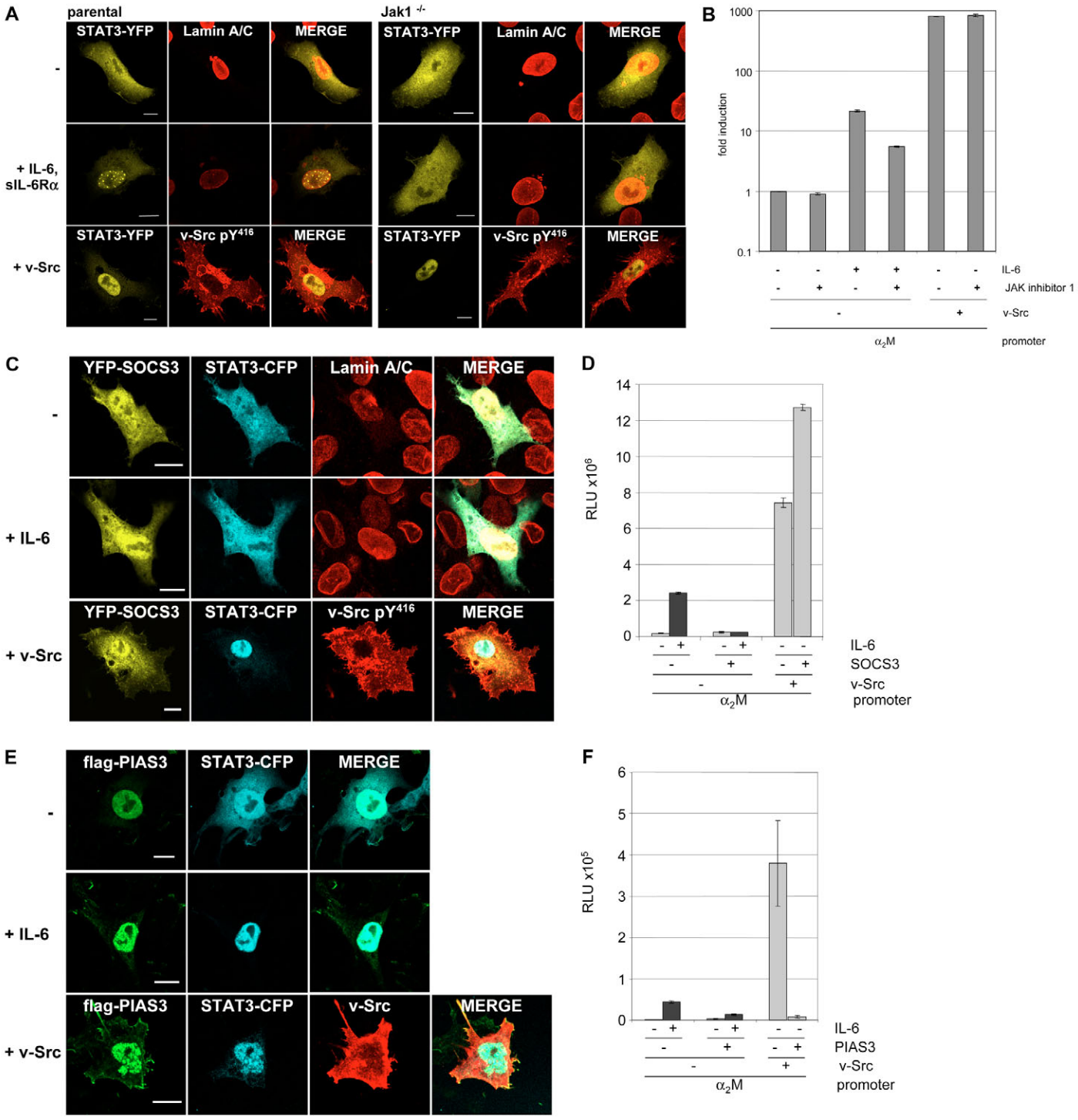

Fig. 2. See next page for legend.

induction of a STAT3-responsive reporter gene by v-Src but affects IL-6 activity (Fig. 2B).

STAT3 activation mediated by gp130 is highly sensitive to suppression by SOCS3 (Schmitz et al., 2000). Therefore, co-transfection of STAT3-CFP and YFP-SOCS3 into HepG2 cells blocks IL-6-induced nuclear translocation of STAT3-CFP (Fig. 2C, middle panel). By contrast, v-Src-mediated nuclear accumulation of STAT3-CFP is not affected by YFP-SOCS3 (Fig. 2C, lower panel). This finding is supported by the results of a reporter gene assay showing that induction of the α2-macroglobulin promoter by v-Src in HepG2 cells is increased rather than inhibited by SOCS3 (Fig. 2D) whereas IL-6-induced α2-macroglobulin induction is strongly downregulated by SOCS3. Taken together, these data suggest that STAT activation through v-Src circumvents Jaks and thereby prevents inhibition by SOCS3.

Fig. 2. Jak1, SOCS3 and PIAS3 in v-Src-mediated STAT3 activation. (A) Parental and Jak1-deficient human fibrosarcoma cells were transiently transfected with STAT3-YFP. Cells were stimulated with 20 ng/ml IL-6 and 1 μg/ml sIL-6Rα for 30 minutes (middle panel) or left unstimulated (upper panel). Cells transiently co-transfected with v-Src were left unstimulated (lower panel). Cells were fixed with paraformaldehyde and, as a nuclear marker, lamin A/C was stained. v-Src was stained with an antibody recognizing pY^{416}-Src. Cells were analyzed by confocal laser-scanning microscopy. Bars, 10 μm. (B) HepG2 human hepatocellular carcinoma cells were transiently transfected with v-Src or with an empty vector. A STAT3-responsive luciferase reporter gene construct under control of the α2M-promoter was co-transfected. Cells were incubated with 20 ng/ml IL-6 or left unstimulated for 24 hours in the presence or absence of 100 ng/ml Jak inhibitor 1 as indicated. Reporter gene assays were performed in triplicate and standard deviations were calculated. (C) HepG2 cells were transiently transfected with YFP-SOCS3 and STAT3-CFP (upper and middle panel) or with YFP-SOCS3, STAT3-CFP and v-Src (lower panel). Stimulation was performed with 20 ng/ml IL-6 for 30 minutes. Fixed cells were stained for lamin A/C or pY^{416}-Src, respectively. Images were taken by confocal laser-scanning microscopy. Bars, 10 μm. (D) HepG2 cells were transiently transfected with SOCS3, v-Src and a α2M reporter gene construct as indicated. Reporter gene assays of IL-6 stimulated (+) and unstimulated (–) cells were performed as described in B. (E) HepG2 cells were transiently transfected with FLAG-PIAS3 and STAT3-CFP (upper and middle panel) or with FLAG-PIAS3, STAT3-CFP and v-Src (lower panel). Stimulation was performed with 20 ng/ml IL-6 for 30 minutes. Fixed cells were stained for FLAG-tagged PIAS3 using a FLAG antibody and an antibody recognizing pY^{416}-Src, respectively. Cells were analyzed by confocal laser-scanning microscopy. Bars, 10 μm. (F) HepG2 cells were transiently transfected with v-Src, FLAG-PIAS3 and a α2M reporter gene construct as indicated. Reporter gene assays were performed as described in D.

PIAS3 has been reported to inhibit gene-induction through activated STAT3 by blocking the DNA-binding activity of the transcription factor (Chung et al., 1997). Nuclear translocation of STAT3-CFP in response to IL-6/sIL-6Rα stimulation or v-Src co-transfection is not altered by co-transfection of FLAG-tagged PIAS3 (Fig. 2E). In contrast to SOCS3, PIAS3 downregulates gene induction mediated by both IL-6 and v-Src (Fig. 2F).

Nucleocytoplasmic shuttling of v-Src-activated STAT3 detected by iFLAP-imaging

Since tyrosine-phosphorylated STATs have been described to undergo rapid dephosphorylation by nuclear phosphatases (Haspel et al., 1996; ten Hoeve et al., 2002), persistent activation of STAT3 requires continuous re-phosphorylation. From our confocal images it is evident that v-Src is excluded from the nucleus (see e.g. Fig. 1E and Fig. 2C). Therefore, reactivation of dephosphorylated STAT3 requires export from the nucleus, re-phosphorylation by v-Src and import into the nucleus, which results in a dynamic equilibrium where nuclear import and nuclear export occur at identical rates. Since the process of nucleocytoplasmic shuttling of STAT3 might be a yet unrecognized target for intervention, we studied this process in more detail.

We used the iFLAP approach (schematically presented in Fig. 3A) to study STAT3 nucleocytoplasmic shuttling in living cells. The upper left image in Fig. 3B shows two HepG2 cells transfected with STAT3-CY. The intensities of CFP and YFP fluorescence along the red line are depicted in the right diagram showing that the cytoplasmic fluorescence is about twice as high as the nuclear fluorescence. The laser intensities and amplifier gain of the confocal microscope were adjusted so that the signal intensities for both fluorophores were identical. This setting represents the equimolar amounts of CFP and YFP in the fusion protein. By the algorithm $I=(1-I_{YFP}/I_{CFP})\times 4096$ (I=signal intensity) the equal signals of CFP and YFP are transformed into zero signal intensity (Fig. 3A, first row and Fig. 3B, second image). A signal is generated by selective bleaching of YFP in a small region of interest (ROI, rectangles in Fig. 3A, second row and Fig. 3B, third image) within the cytoplasm of the cell. The signal that rapidly spreads within the cytoplasm represents freely diffusing STAT3 molecules with intact CFP fluorescence and destroyed YFP fluorescence. After 5 minutes the first signals appear within the nucleus and slowly increase during the following 15 minutes (Fig. 3B). The nuclear signal arises from constitutive nucleocytoplasmic shuttling of STAT3-CY, i.e. YFP-bleached STAT3-CY enters the nucleus and this flow is compensated by export of non-bleached STAT3-CY. The weak signals emerging from the second cell only marginally increase during the time series indicating that bleaching by data recording is negligible.

The same experiment was performed in cells co-transfected with STAT3-CY and v-Src. Double-transfected cells are characterized by an increased nuclear fluorescence signal (Fig. 3C, first image and diagram). Cytoplasmic bleaching resulted in an accelerated increase in the nuclear signal compared with cells transfected with STAT-CY alone (compare Fig. 3B with C; see also Movies 1 and 2 in the supplementary material) indicating that STAT3 constitutively activated by v-Src shuttles more rapidly between the cytoplasm and nucleus than non-phosphorylated STAT3. When the same experiment as depicted in Fig. 3C is performed in the presence of the nuclear export inhibitor ratjadone A (Köster et al., 2003), continuous bleaching of YFP in the cytoplasm results in only a low nuclear signal (Fig. 3D). Thus, blockade of exportin-1-mediated nuclear export results in decreased nucleocytoplasmic shuttling of constitutively activated STAT3-CY.

Quantitative analysis of STAT3 nucleocytoplasmic shuttling by iFLAP combined with mathematical modelling

In the iFLAP experiments, variation of the experimental parameters is inevitable from one single cell experiment to the next. This variation results, for example, from different cell shapes or changing levels of STAT3-CY expression, leading to different degrees of initial YFP bleaching. For these reasons, a direct quantitative comparison of the fluorescence intensity time series for wild-type and v-Src-transfected cells is difficult, if not impossible, although visual inspection of the data suggests that differences exist between the shuttling dynamics in wild-type and v-Src-transfected cells (Fig. 3).

In order to compare nucleocytoplasmic shuttling of non-activated and persistently activated STAT3 more rigorously, iFLAP data were generated that are suited for quantitative evaluation with a mathematical model for the dynamics of nucleocytoplasmic shuttling. The procedure adapted from our previous work (Pranada et al., 2004) is exemplified in Fig. 4A showing two HepG2 cells transfected with STAT3-CY, the

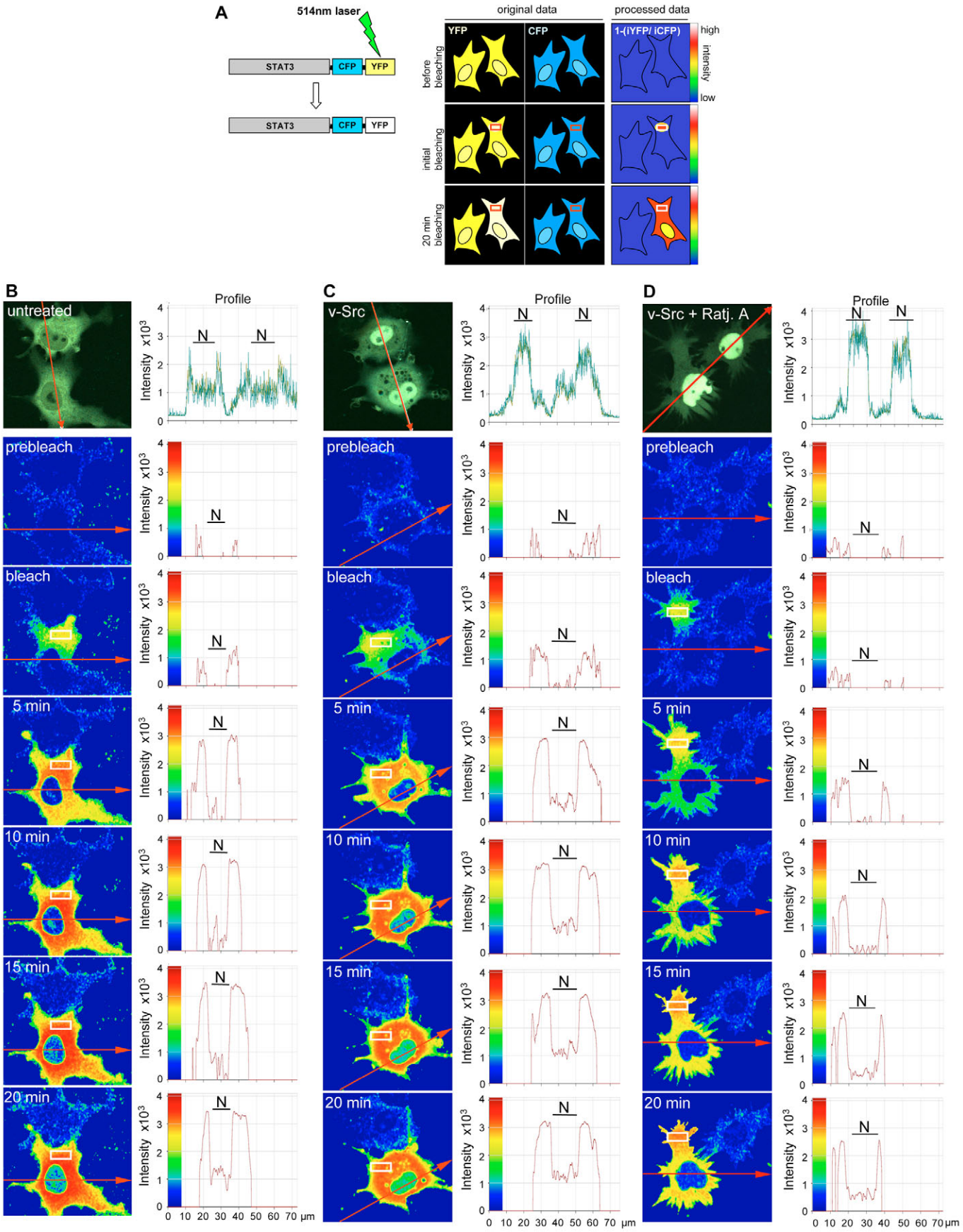

Fig. 3. See next page for legend.

Fig. 3. iFLAP imaging. (A) Schematic representation of the iFLAP imaging approach. (Left) Using the 514 nm laser of the confocal laser-scanning microscope the YFP part of STAT3-CY can be selectively bleached. (Right) The images of STAT-CY in the YFP and CFP channels of the confocal microscope (original data) are processed into zero signal intensity depicted as blue (intensity= 1–(iYFP/iCFP). Selective bleaching of YFP within the rectangular bleaching-ROI (ROI=region of interest) generates a subpopulation of STAT3-CY molecules that are only detected in the CFP-channel. These molecules generate a signal in the processed data channel. They diffuse freely through the cytoplasm and finally appear within the nucleus. (B) HepG2 transiently transfected with STAT3-CY were analyzed in a perfusion chamber for live cell imaging at the confocal laser-scanning microscope. Two neighbouring cells were selected for imaging (upper-left image shows the merged YFP and CFP channels). The YFP and CFP fluorescence along the red line are shown in the upper-right diagram as yellow and blue graphs, respectively (N, fluorescence intensity within the nucleus). The lower cell was selected for the iFLAP experiment. A bleaching-ROI (white rectangle) was placed into its cytoplasmic compartment, the bleaching procedure was performed, and fluorescence intensity signals of both CFP and YFP were recorded every 5 minutes. Detected signals were recalculated by using the algorithm described in A to generate a signal that represents the distribution of the bleached subpopulation of STAT3-CY over time. As a control the second cell was monitored without bleaching. Relative fluorescence is depicted in false colour mode corresponding to its intensities. Fluorescence intensity profiling (red arrows and right diagrams) is depicted to show the increasing signal in the nuclear compartment. (C) The same experiment was performed as described in B with HepG2 cells coexpressing STAT3-CY and v-Src. (D) The same experiment was performed as described in C in the presence of 100 ng/ml ratjadone A.

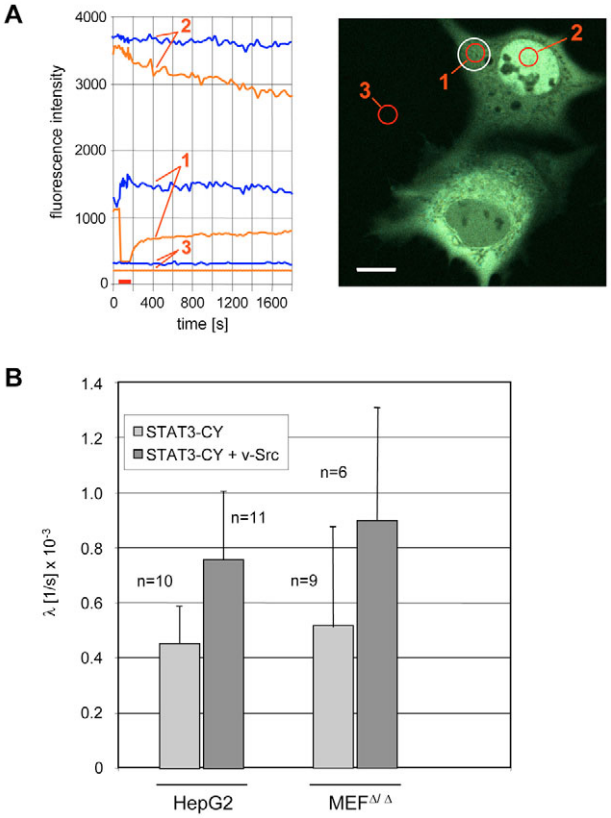

Fig. 4. Quantitative iFLAP. (A) HepG2 cells co-transfected with STAT3-CY and v-Src were analyzed in a perfusion chamber for live cell imaging at the confocal microscope. CFP and YFP fluorescence intensities were monitored exclusively in regions of interest (ROI, numbered red circles in the images) over time. The initial cytoplasmic bleaching was performed in the bleach ROI (white circle) over the time indicated by the red bar on the *x*-axis in the diagram. The diagram represents the mean CFP (blue lines) and YFP fluorescence intensities (orange lines) in the three ROIs over time. The red numbers in the diagrams correspond to the cytoplasmic (1), nuclear (2) and background (3) detection ROIs. A representative experiment is shown. (B) iFLAP experiments were performed with HepG2 cells transiently transfected with STAT3-CY and with stably transfected $MEF^{\Delta/\Delta}$-STAT3-CY cells co-transfected with v-Src or empty vector as described in A. The resulting curves were analyzed by mathematical modelling and computational parameter estimation. The bar chart depicts the mean values and s.d. of the exponential coefficient λ as a measure for the rate of shuttling.

upper one being co-transfected with v-Src. In the marked ROIs (red circles) cytoplasmic, nuclear and background fluorescence are measured in small, defined areas with high temporal resolution. Initial pulse-bleaching with the 514 nm laser in the bleach ROI (white circle) leads to a sharp decrease in cytoplasmic YFP fluorescence. By contrast, the CFP fluorescence remains unaffected over time with the exception of an initial increase after cytoplasmic YFP bleaching owing to the loss of FRET between CFP and YFP (Fig. 4A, curves 1). After bleaching is stopped, nuclear YFP fluorescence slowly decreases, whereas nuclear CFP fluorescence remains constant (Fig. 4A, curves 2). This is indicative for nucleocytoplasmic shuttling of STAT3-CY.

In order to quantitatively compare shuttling dynamics of STAT3-CY in the presence or absence of v-Src, a differential equation model was derived as briefly described in the Materials and Methods. Combining iFLAP data recorded as shown in Fig. 4A and in silico maximum-likelihood parameter estimation, biologically relevant model parameters for the shuttling dynamics can be determined quantitatively for each cell subjected to an iFLAP experiment. Based on these model parameter values, a quantitative analysis of STAT3 shuttling under different conditions becomes possible by comparison of the resulting exponential coefficients λ (see Eqn 3 below). The results summarized in Fig. 4B (left columns) show that STAT3 shuttling is more rapid in the v-Src-transfected HepG2 cells (λ=0.000758±0.000295 $seconds^{-1}$, half-life of recovery τ=914±356 seconds) compared with HepG2 cells transfected with STAT3-CY alone (λ=0.000450±0.000141 $seconds^{-1}$, τ=1540±483 seconds). The same experiments were performed with $MEF^{\Delta/\Delta}$ cells stably transfected with STAT3-CY (Fig. 4B, right columns; λ=0.000534±0.000354 $seconds^{-1}$, τ=1299±862 seconds). Again, co-transfection of v-Src accelerates nucleocytoplasmic shuttling (λ=0.000911±0.000416 seconds, τ=761±347 seconds).

Inhibition of nucleocytoplasmic shuttling leads to a decrease in v-Src-induced STAT3 phosphorylation and STAT3-mediated gene induction

Since tyrosine-phosphorylated STAT3 is rapidly inactivated by nuclear phosphatases (ten Hoeve et al., 2002), we assumed that nucleocytoplasmic shuttling is a prerequisite for persistent activation by the membrane-associated v-Src kinase. Ratjadone

A treatment of IL-6/sIL-6Rα-stimulated MEF$^{\Delta/\Delta}$STAT3-YFP cells leads to a prolonged nuclear accumulation of STAT3-YFP (Fig. 5A, upper panel), as has been observed upon leptomycin B treatment (Bhattacharya and Schindler, 2003) because exportin-1-mediated nuclear export is inhibited. After 240 minutes of IL-6 stimulation in the presence of ratjadone A there is as much STAT3 in the nucleus as after 30 minutes of IL-6 stimulation in the absence of ratjadone (Fig. 5A, upper panel). However, the tyrosine phosphorylation at the corresponding time points is strongly reduced following ratjadone A treatment (Fig. 5A lower panel). This finding suggests dephosphorylation of nuclear STAT3 in the presence of ratjadone A. The tyrosine phosphorylation does not completely vanish because there is still a substantial cytoplasmic fraction of STAT3 left that is prone to phosphorylation by activated receptors. Ratjadone A treatment

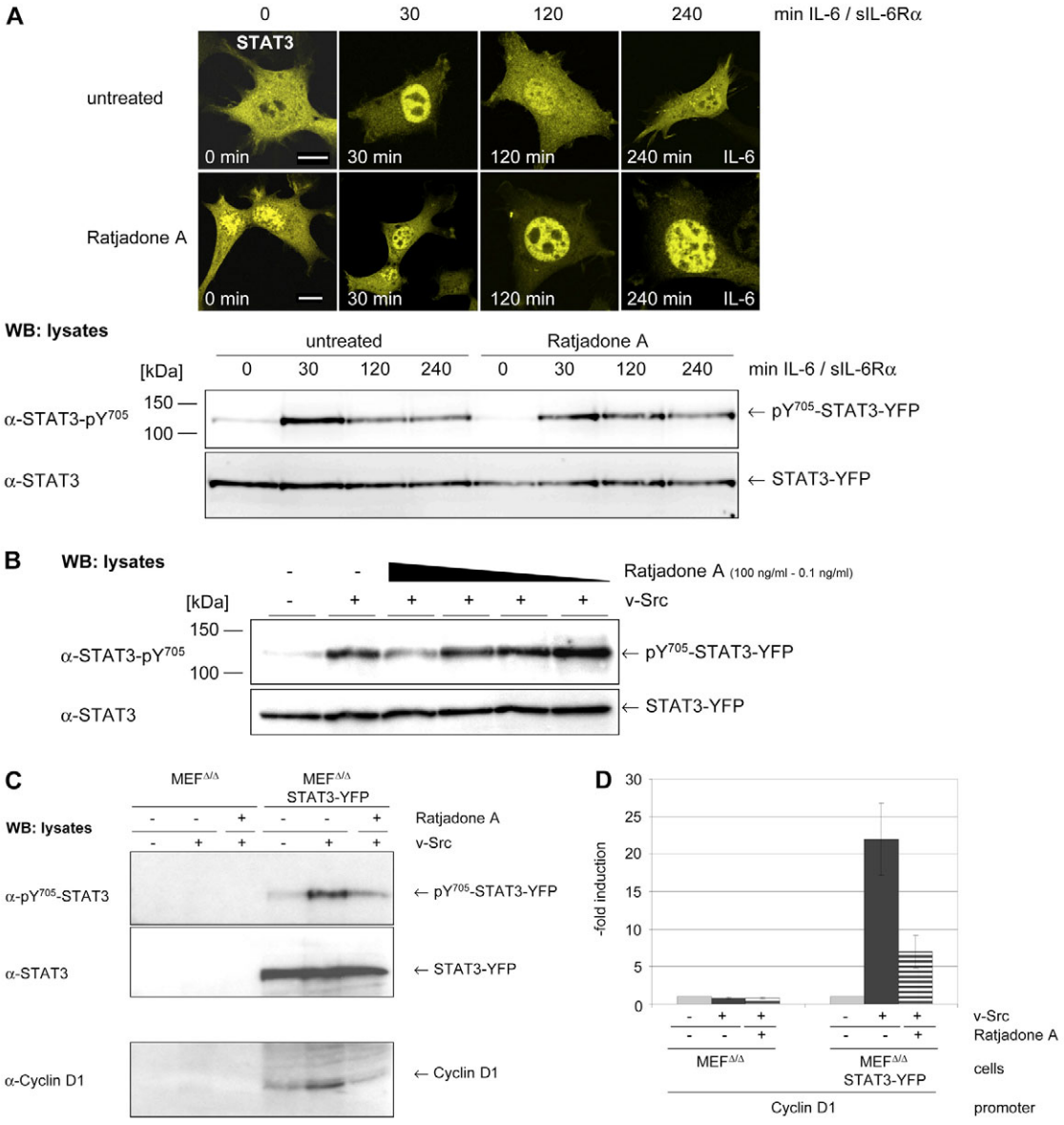

Fig. 5. Inhibition of nuclear export leads to a decrease in v-Src-mediated STAT3 activation and gene induction. (A) MEF$^{\Delta/\Delta}$STAT3-YFP cells were stimulated with 20 ng/ml IL-6 and 0.5 μg/ml sIL-6Rα for the indicated times and treated with 100 ng/ml ratjadone A (lower panel) or left untreated (upper panel). Fixed cells were analyzed by confocal laser-scanning microscopy. Bars, 10 μm. A western blot of corresponding lysates of MEF$^{\Delta/\Delta}$STAT3-YFP cells was analyzed for pY^{705}-STAT3 and counterstained for total STAT3. (B) MEF$^{\Delta/\Delta}$STAT3-YFP cells were transfected with v-Src and treated for 2 hours with ratjadone A as indicated. Whole cell lysates were subjected to SDS-PAGE and western blotting. STAT3 tyrosine phosphorylation was detected with a pY^{705}-STAT3 antibody. For loading control the blot was stained with a STAT3 antibody. (C) MEF$^{\Delta/\Delta}$ cells and MEF$^{\Delta/\Delta}$STAT3-YFP cells were transfected with v-Src and treated with ratjadone A for 24 hours. Cell lysates were subjected to SDS-PAGE and western blotting. pY^{705}-STAT3, STAT3 and cyclin D1 were detected by immunostaining. (D) A luciferase reporter construct under control of the cyclin D1 promoter was transfected into MEF$^{\Delta/\Delta}$ and MEF$^{\Delta/\Delta}$STAT3-YFP cells. v-Src was co-transfected as indicated. 48 hours after transfection cells were treated with 100 ng/ml ratjadone A for 24 hours or left untreated. Reporter gene assays were performed in triplicate and s.d. was calculated.

of MEF$^{\Delta/\Delta}$STAT3-YFP cells transiently co-transfected with v-Src results in a dose-dependent decrease in STAT3-YFP tyrosine phosphorylation (Fig. 5B) indicating that trapping of STAT3 in the nucleus leads to its dephosphorylation by nuclear phosphatases. Thus, inhibition of nucleocytoplasmic shuttling reduces the amount of activated STAT3 in the nucleus.

Cyclins D1 and D2 are among the STAT3 target genes dysregulated in malignant transformation by v-Src (Sinibaldi et al., 2000). Accordingly, v-Src transfection into MEF$^{\Delta/\Delta}$STAT3-YFP cells leads to an induction of cyclin D1 whereas in STAT3-knockout cells no cyclin D1 induction upon v-Src expression is detectable (Fig. 5C). Most importantly, induction of cyclin D1 is reduced by treatment of cells with ratjadone A. This observation made with the endogenous cyclin D1 (Fig. 5C) and D2 (not shown) genes in MEF cells is supported by a reporter gene assay. STAT3-YFP is required for the induction of a luciferase reporter gene under the control of the cyclin D1 promotor (Fig. 5D). Gene induction is strongly suppressed by treatment of the cells with ratjadone A.

Increased sensitivity of v-Src-transformed fibroblasts towards inhibition of nuclear export

Induction of proliferative and anti-apoptotic genes by persistently activated STAT3 is a requirement for transformation of fibroblasts by v-Src (Bromberg et al., 1998; Schlessinger and Levy, 2005). We asked the question whether v-Src transformed fibroblasts are more sensitive to the blockade of nuclear export than fibroblasts transformed by the 3T3 protocol. Analysis of nuclear and cytoplasmic fractions of both cell lines confirmed that v-Src transformed fibroblasts contain much more tyrosine-phosphorylated STAT3 in their nuclei than NIH3T3 fibroblasts (data not shown). v-Src-transformed fibroblasts and NIH3T3 fibroblasts were cultured for 72 hours. Visual inspection of the cells (Fig. 6A) revealed that NIH3T3 fibroblasts withstand ratjadone A treatment during the last 24 hours of culture whereas fewer v-Src-transformed cells survived with many of them showing an apoptotic phenotype. When cells were treated with ratjadone A for 24 hours and the block of nuclear export was then released for the last 24 hours, most of the v-Src-transformed fibroblasts died whereas many of the 3T3 fibroblasts survived.

The above cells were harvested after 72 hours and analyzed for STAT3 tyrosine phosphorylation and induction of apoptosis. In v-Src-transformed fibroblasts, a strong tyrosine phosphorylation of STAT3 was detected whereas in NIH3T3 fibroblasts STAT3 phosphorylation was rather weak (Fig. 6B). Treatment with ratjadone A for the last 24 hours of culture strongly reduced STAT3 phosphorylation in both cell types. After release of 24 hours export block during the last 24 hours of culture NIH3T3 fibroblasts recovered. Neither STAT3

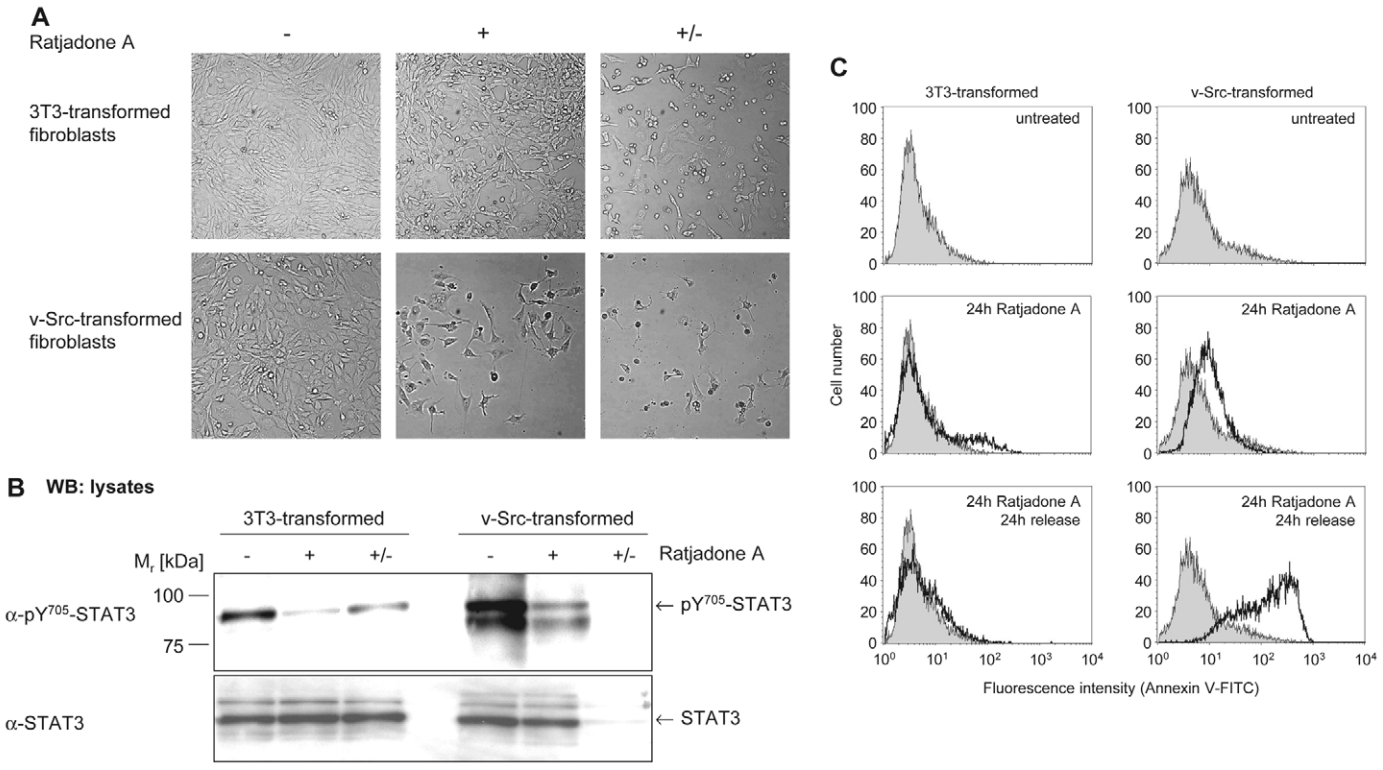

Fig. 6. Disrupting nucleocytoplasmic shuttling of constitutively activated STAT3 in v-Src-transformed fibroblasts results in apoptotic cell death. Mouse 3T3 fibroblasts and v-Src-transformed mouse fibroblasts were cultivated in six-well plates for 72 hours and then subjected to further analysis. Cells were either left untreated (–), were treated with ratjadone A for the last 24 hours (+) or treated with ratjadone for 24 hours and subsequently incubated for another 24 hours without ratjadone A (+/–). (A) Phase contrast images of the cells after 72 hours. (B) Cell lysates were subjected to SDS-PAGE and western blotting. pY^{705}-STAT3 and STAT3 were detected by immunostaining. (C) Cells were harvested, stained with annexin V-FITC and analyzed by flow cytometry. The non-treated cell population is shown in grey in all histograms. The histograms of ratjadone-A-treated cells are shown as black lines.

phosphorylation nor STAT3 protein was detectable in the residual v-Src-transformed fibroblasts.

Induction of apoptosis was detected by annexin V staining of the cells and subsequent FACS analysis (Fig. 6C). 24 hours of ratjadone treatment resulted in a shift of the whole population of v-Src-transformed fibroblasts whereas only a minor portion of the NIH3T3 fibroblasts was annexin V positive. After 24 hours of recovery from ratjadone A treatment, no apoptosis induction was detected in the surviving NIH3T3 fibroblasts whereas the v-Src-transformed fibroblasts were strongly annexin V positive indicating progression of apoptosis.

Taken together, a block of exportin-1-mediated nuclear export leads to reduced nucleocytoplasmic shuttling of STAT3. Consequently, v-Src-induced STAT3 phosphorylation and STAT3-mediated gene expression is decreased resulting in irreversible induction of apoptosis in v-Src-transformed cells.

Discussion

Although activation of STAT3 through cytokine receptors is transient, persistent activation of STAT3 has been detected in many types of cancer (Yu and Jove, 2004). The mechanism of constitutive STAT3 activation by v-Src has been studied in some detail. It has been shown that v-Src phosphorylates and activates Jak1, which suggests that Jak-1 contributes to the v-Src-induced phosphorylation of STAT3 (Zhang et al., 2000b). However, there is strong evidence for an interaction of STAT3 and v-Src leading to direct phosphorylation of STAT3 by v-Src (Cao et al., 1996; Zhang et al., 2000a). In order to clarify the mechanism underlying the constitutive STAT3 activation we coexpressed STAT3-YFP or STAT3-CY with v-Src. We found that phosphorylation by v-Src requires the intact SH2-domain of STAT3, which suggests that canonical cytokine receptor/Jak signalling might be involved. However, deletion or inhibition of Jaks does not block phosphorylation of STAT3 by v-Src. As a consequence, the STAT3-induced feedback inhibitor SOCS3, which interferes with STAT3 activation through cytokine receptors and Jaks, does not inhibit STAT3 activation by v-Src. Compared with the SOCS3 feedback-controlled IL-6 mediated activation, the uncontrolled activation of STAT3 by v-Src leads to a much stronger gene induction. The massive gene induction evoked by persistently activated STAT3 might contribute to tumour progression. PIAS3, the protein inhibitor of activated STAT3, does not discriminate between STAT3 phosphorylated by v-Src or by the canonical gp130/Jak1 pathway (summarized in Fig. 7). The function of the STAT3 SH2-domain in activation by v-Src is still unresolved. Possibly, a direct phosphorylation of STAT3 by v-Src is mediated by an SH2-domain/phosphotyrosine interaction.

v-Src is myristoylated and bound to the cytoplasmic leaflet of membranes and thereby excluded from the nucleus. Thus, the cytoplasm can be regarded as the cellular STAT3 activation compartment. Conversely, the nucleus can be considered to be the STAT3 inactivation compartment, since STAT3 dephosphorylation at pY705 occurs mainly here. In this context, persistent activation of STAT3 requires a cyclic process of phosphorylation in the cytoplasm, transfer through the nuclear pore complex (NPC), dephosphorylation in the nucleus and export through the NPC (Fig. 7, left). Although this continuous reactivation cycle of STAT3 has been postulated (Darnell, 2005), it has not been directly demonstrated or quantified. Alternative mechanisms for enhanced STAT3 activation in v-Src-transformed cells could be thought of. For example, v-Src transformation of cells could interfere with the dephosphorylation of STAT3 in the nucleus and thereby prevent inactivation and export of nuclear STAT3. In this static model of STAT3 activation by v-Src, nucleocytoplasmic shuttling of STAT3 would not play a role.

We detected nucleocytoplasmic shuttling of activated STAT3 by iFLAP-imaging. Nucleocytplasmic shuttling reflects a dynamic steady state with constitutive nuclear import and export occurring at identical rates. Using the iFLAP approach, mathematic modeling, and in silico parameter estimation, we were able to compare rates of nucleocytoplasmic shuttling of

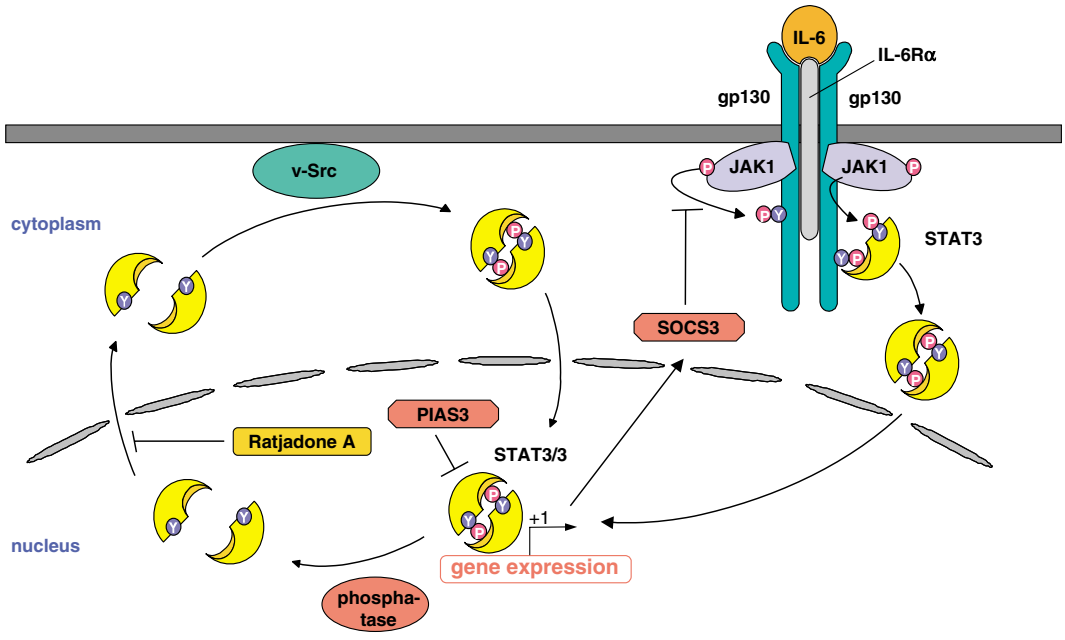

Fig. 7. v-Src- and IL-6-mediated STAT3 activation and its inhibition. Cytokine-induced STAT3 activation (right) is transient owing to the induction of the feedback inhibitor SOCS3. Persistent activation of STAT3 by v-Src (left) requires nucleocytoplasmic shuffling. Inhibition of nuclear export blocks the reactivation cycle. See Discussion for details.

cells with non-activated STAT3 to those of cells with persistently activated STAT3 quantitatively. We found that nucleocytoplasmic shuttling of activated STAT3 is about 1.7-fold more rapid in comparison with non-activated STAT3. What is the mechanism behind the v-Src-induced acceleration of STAT3 nucleocytoplasmic shuttling? Tyrosine phosphorylation of STAT3 leads to its interaction with importins α5 and α7 resulting in a facilitated nuclear import whereas non-phosphorylated STAT3 does not interact with importins (Ma and Cao, 2006). The slow importin-independent shuttling of non-phosphorylated STAT3 (Fig. 3B) (Pranada et al., 2004) might be mediated either by direct interaction with the NPC as it has been described for STAT1 (Marg et al., 2004) or by a general slow leakage of cytoplasmic proteins into the nucleoplasm (Mingot et al., 2004).

After dephosphorylation by TC45, the nuclear isoform of the T-cell protein tyrosine phosphatase (TC-PTP) (ten Hoeve et al., 2002), STAT3 is a substrate for exportin-1/crm-1 mediated export (Bhattacharya and Schindler, 2003). Indeed, upon treatment of v-Src-transfected cells with the exportin-1 inhibitor ratjadone A, we found that nucleocytoplasmic shuttling of activated STAT3 slows down leading to a trapping of STAT3 in the nucleus (Fig. 3D). Retention of activated STAT3 in the inactivation compartment is accompanied by a reduction of tyrosine phosphorylation. As a result, the induction of STAT3 target genes such as cyclins D1 and D2 decreases (Fig. 5). For the related protein STAT5, it has been shown that the transient canonical activation through cytokine receptors also requires continuous reactivation at the receptor (Swameye et al., 2003; Zeng et al., 2002). Thus, in cancer types where persistent activation of STATs is achieved by autocrine or paracrine cytokine or growth factor stimulation, inhibition of nuclear export should also lead to inactivation.

Transformation of fibroblasts by v-Src requires gene induction by activated STAT3 (Bromberg et al., 1998; Schlessinger and Levy, 2005). STAT3 prevents apoptosis by upregulation of Bcl-2 and Mcl-1 and downregulation of p53 (Niu et al., 2005). We found that v-Src-transformed fibroblasts are highly sensitive to inhibition of the STAT3 reactivation cycle by the blockade of nuclear export. Ratjadone A treatment led to loss of STAT3 tyrosine phosphorylation and apoptotic cell death. The weak STAT3 tyrosine phosphorylation detected in NIH3T3 fibroblasts was also affected by ratjadone A treatment. However, in cells transformed by the 3T3 protocol, STAT3 activation seems not to be essential for survival.

Persistently activated STAT3 is a promising target in cancer therapy. Several approaches have concentrated on the inhibition of the activating kinases including overexpression of SOCS proteins (Darnell, 2005). The latter approach might only work in those special cases where Jaks are involved. It will fail when the activating kinase such as v-Src is not inhibited by SOCS proteins. Attempts to target STAT3 directly were based on its knock-down by siRNA, overexpression of dominant negative STAT3 or application of peptide inhibitors that interfere with STAT3 dimerization (Darnell, 2005; Yu and Jove, 2004). Transit of STAT3 through the NPC has not been considered yet as a target for intervention. We propose that the somewhat counterintuitive approach of trapping an oncogenic transcription factor within the nuclear compartment is a promising new facet in the attempts to inactivate STAT3. Of course, a general block of nuclear export would not target the cancer cell alone but would have severe side effects on healthy cells. Therefore, the structural determinants for nuclear export of STAT3 have to be defined in more detail to become specific targets for intervention.

Materials and Methods

Recombinant plasmids

The expression vectors pSVL-STAT3-YFP, pSVL-STAT3-CFP, and pSVL-STAT3-CY were generated as described previously (Herrmann et al., 2004; Pranada et al., 2004). pSVL-STAT3-YFP was used as a template for cloning the constructs pSVL-STAT3(321-771)-YFP, pSVL-STAT3(R609Q)-YFP, pSVL-STAT3(Y705F)-YFP and pcDNA5/FRT/TO-STAT3-YFP by PCR. The plasmids pM-v-Src and pCMV-FLAG-PIAS3 were generous gifts of James Turkson (University of Central Florida, USA) and K. Shuai (University of Los Angeles, USA), respectively. R. Morriggl (Ludwig Boltzmann Institut, Vienna, Austria) kindly provided the plasmids pcDNA3-huFyn and pMSCV-BCR/Abl-IRES-GFP; pLNCX-Abl was provided by P. Rothman (University of Iowa, USA). The expression vector pEF-YFP-SOCS3 was constructed by fusing YFP to the N-terminus of SOCS3. A reporter plasmid with the promoter for α_2-macroglobulin (α_2M) has been described previously (Herrmann et al., 2004). The cyclin D1-promoter fused to the luciferase gene was a kind gift of B. Lüscher (University of Aachen, Germany).

Cell culture and transfection

COS-7 simian monkey kidney cells, human fibrosarcoma cells (2C4, U4C, γ2A, U1A) (kindly provided by I. M. Kerr, Cancer Research UK, London), murine embryonal fibroblast ($MEF^{fl/fl}$, $MEF^{\Delta/\Delta}$) (Costa-Pereira et al., 2002), NIH3T3 mouse fibroblasts, and v-Src-transformed mouse fibroblasts (generous gift of M. Kortylewski, Beckman Research Institute, Los Angeles, CA) were grown in Dulbecco's Modified Eagle Medium (DMEM), HepG2 cells in DMEM/F12, both supplemented with 10% FCS, 100 U/ml penicillin and 100 μg/ml streptomycin (BIO-Whittaker, Verviers, Belgium). Cells were grown at 37°C in a water-saturated atmosphere at 5% CO_2. $MEF^{\Delta/\Delta}$ cells were stably reconstituted with STAT3-YFP or STAT3-CY using the Flp-In technique (Invitrogen). Transient transfections were performed by using the DEAE-dextrane method for COS-7 cells. FuGENE 6 transfection reagent (Roche, Mannheim, Germany) was used according to the manufacturer's instruction for transfection of HepG2 and MEF cells. Fibrosarcoma cells were transfected using Superfect (Qiagen, Hilden, Germany). Treatment of cells with ratjadone A (generous gift of Mario Köster and Hansjörg Hauser, GBF, Braunschweig, Germany) was performed as described in the figure legends.

Chemicals and antibodies

DMEM and DMEM/F12 were purchased from GIBCO (Invitrogen), FCS from CytoGen (Sinn, Germany). GFP antibodies were obtained from Rockland Immunochemicals (Philadelphia, PA), pY^{705}-STAT3 antibody from Cell Signaling Technology (Danvers, MA), antibodies raised against STAT3, Cyclin D1, Lamin A/C from Santa Cruz Biotechnology (Santa Cruz, CA), pY^{418}Src (Biosource, CA), αFLAG (Sigma). Fluorescently labelled antibodies were obtained from Jackson Immunolaboratories; HRP conjugated secondary antibodies were purchased from Dako (Hamburg, Germany). Jak inhibitor 1 was purchased from Calbiochem (Darmstadt, Germany).

Immunoprecipitation and western blotting

Immunoprecipitations from total cell lysates using a GFP-antibody were performed as described (Herrmann et al., 2004). Precipitated proteins were separated by SDS-PAGE and transferred to PVDF-membranes (PALL, Dreieich, Germany) by semi-dry blotting. After blocking with 10% BSA the membrane was incubated with the antibodies as indicated and processed for chemiluminescence detection (ECL, Amersham, Uppsala, Sweden).

Electrophoretic mobility shift assay (EMSA)

EMSA was performed as described previously (Herrmann et al., 2004) using a [α-^{32}P]-labelled, double-stranded oligonucleotide derived from a mutated sis-inducible element (SIE) of the *c-fos* promotor (m67SIE: GAT CCG GGA GGG ATT TAC GGG AAA TGC TG). For supershifts, the radioactively labelled probe and nuclear extracts were incubated with 1 μg STAT3 antibody or 1 μg GFP antibody for 10 minutes.

Indirect immunofluorescence

Immunofluorescence staining of cells was carried out after formaldehyde fixation as described (Herrmann et al., 2004). Indicated primary and secondary antibodies were used at a 1:100 dilution. Slides were mounted with Mowiol (Calbiochem, USA).

Confocal microscopy and live cell imaging

Confocal imaging was carried out on a Zeiss LSM 510Meta confocal microscope (Zeiss, Jena, Germany). Cy3-fluorescence was excited using the 543 nm emission line of the helium-neon laser, a 543 nm dichroic mirror and a 560-600 nm bandpass

filter. Cy2-fluorescence was detected using the 488 nm emission line of the argon laser, a 488 nm dichroic mirror and a 505-530 nm bandpass filter. CFP and YFP signals were detected as described previously (Pranada et al., 2004). The images shown represent confocal slices of approximately 1 μm. Cells were examined with a 63× 1.2 NA Zeiss water immersion objective.

Live cell experiments were carried out with transiently transfected HepG2 cells or stably transfected MEF cells. Transfected cells were grown on 42 mm glass coverslips. After 48 hours the coverslips were placed into a thermostat-controlled (37°C) and CO_2-controlled perfusion chamber (Pecon, Erbach, Germany) and flushed with Krebs-Ringer-Hepes buffer (130 mM NaCl, 4.7 mM KCl, 2.5 mM $CaCl_2$, 1.2 mM KH_2PO_4, 1.2 mM $MgSO_4$, 5.5 mM glucose, 10 mM HEPES, pH 7.4). Quantitative iFLAP was performed as described previously (Pranada et al., 2004). For iFLAP imaging the CFP and YFP signals from STAT3-CY were adjusted to equal intensities. An iFLAP signal was generated by bleaching the YFP moiety in a cytoplasmic ROI with the 514 nm line of the argon laser during data recording. Depicted intensities were calculated using the algorithm $I=(1-I_{YFP}/I_{CFP})\times 4096$.

Reporter gene assay

For reporter gene assays, usually 1 μg of reporter plasmid was co-transfected into HepG2 or MEF cells together with 2 μg pM-v-Src alone or 1 μg pM-v-Src and 500 ng pEF-YFP-SOCS3 or 1.5 μg pCMV-FLAG-PIAS3, respectively. A plasmid encoding β-galactosidase was co-transfected to control transfection efficiency. Cells were cultured for 48 hours and subsequently prepared for measurement of luciferase and β-galactosidase activity. All experiments were performed in triplicate and standard deviations were calculated.

Apoptosis assay

Mouse 3T3 fibroblasts and v-Src-transformed mouse fibroblasts were grown in six well plates. After treatment with 100 ng/ml Ratjadone A diluted in culture media, cells were washed twice with ice-cold PBS and subsequently harvested with PBS supplemented with EDTA. Apoptosis tests were performed with the Annexin V-FITC Apotosis Detection Kit I (BD Pharmingen) according to the manufacturer's instructions.

Mathematical modeling and parameter estimation

Mathematical modeling was carried out in terms of normalized intensities:

$$J_i(t) = I_i(t)/I_i(0) \qquad i = c,n\ , \tag{1}$$

where $I_i(t)$ refers to the intensity measured at time t in a quantitative FLAP experiment for any time point t after bleaching is switched off, $t>t_{off}$, and $I_i(0)$ denotes the intensity before bleaching. In Eqn 1 the indices $i=c$ and n refer to the cytoplasm and nucleus, respectively. Assuming that a dynamic steady state of nuclear and cytoplasmic STAT3 concentrations results from balancing flows of STAT3 from the cytoplasm to the nucleus and vice versa, the following simple dynamical model can be derived for the normalized intensities:

$$\dot{J}_c = k_c(J_n - J_c) \qquad J_c(t_{off}) = J_{c,off}\ , \tag{2a}$$

$$\dot{J}_n = k_n(J_c - J_n) \qquad J_n(t_{off}) = J_{c,off}\ . \tag{2b}$$

In Eqn 2a and 2b, $J_{c,off}$ and $J_{n,off}$ refer to the normalized cytoplasmic and nuclear intensities at the time when bleaching is turned off. Owing to their simplicity, the equations can be solved analytically to give:

$$J_i = \alpha_i \exp(-\lambda t) + \beta \qquad i = n,c\ , \tag{3}$$

where $\lambda=k_n+k_c$. According to Eqn 3, J_n and J_c decay to a common equilibrium value β for $t\rightarrow\infty$. Since λ determines the rate of decay, larger values of λ indicate a faster decay to this new equilibrium by nucleocytoplasmic shutling after bleaching. The value of λ cannot be determined from the FLAP data directly. In order to determine λ, we carried out maximum-likelihood parameter estimations by solving least-squares optimization problems with a gradient-based optimization algorithm. According to $\tau=\ln 2/\lambda$, the half-life τ is a measure for the half-life of fluorescence decay in the nucleus after cytoplasmic bleaching.

This work was supported by the Deutsche Forschungsgemeinschaft (SFB 542, projects B12 and Z1 to G.M.-N.), the Fonds der Chemischen Industrie (to P.C.H.) and the Italian Association for Cancer Research AIRC (to V.P.). The authors thank Hildegard Schmitz-van de Leur for excellent technical assistance.

References

Bhattacharya, S. and Schindler, C. (2003). Regulation of Stat3 nuclear export. *J. Clin. Invest.* **111**, 553-559.

Bromberg, J. F., Horvath, C. M., Besser, D., Lathem, W. W. and Darnell, J. E., Jr (1998). Stat3 activation is required for cellular transformation by v-src. *Mol. Cell. Biol.* **18**, 2553-2558.

Cao, X., Tay, A., Guy, G. R. and Tan, Y. H. (1996). Activation and association of Stat3 with Src in v-Src-transformed cell lines. *Mol. Cell. Biol.* **16**, 1595-1603.

Chung, C. D., Liao, J., Liu, B., Rao, X., Jay, P., Berta, P. and Shuai, K. (1997). Specific inhibition of Stat3 signal transduction by PIAS3. *Science* **278**, 1803-1805.

Costa-Pereira, A. P., Tininini, S., Strobl, B., Alonzi, T., Schlaak, J. F., Is'harc, H., Gesualdo, I., Newman, S. J., Kerr, I. M. and Poli, V. (2002). Mutational switch of an IL-6 response to an interferon-gamma-like response. *Proc. Natl. Acad. Sci. USA* **99**, 8043-8047.

Darnell, J. E. (2005). Validating Stat3 in cancer therapy. *Nat. Med.* **11**, 595-596.

Haspel, R. L., Salditt-Georgieff, M. and Darnell, J. E., Jr (1996). The rapid inactivation of nuclear tyrosine phosphorylated Stat1 depends upon a protein tyrosine phosphatase. *EMBO J.* **15**, 6262-6268.

Heinrich, P. C., Behrmann, I., Haan, S., Hermanns, H. M., Müller-Newen, G. and Schaper, F. (2003). Principles of interleukin (IL)-6-type cytokine signalling and its regulation. *Biochem. J.* **374**, 1-20.

Herrmann, A., Sommer, U., Pranada, A. L., Giese, B., Küster, A., Haan, S., Becker, W., Heinrich, P. C. and Müller-Newen, G. (2004). STAT3 is enriched in nuclear bodies. *J. Cell Sci.* **117**, 339-349.

Itoh, M., Murata, T., Suzuki, T., Shindoh, M., Nakajima, K., Imai, K. and Yoshida, K. (2005). Requirement of STAT3 activation for maximal collagenase-1 (MMP-1) induction by epidermal growth factor and malignant characteristics in T24 bladder cancer cells. *Oncogene* **25**, 1195-1204.

Iwamoto, T., Senga, T., Naito, Y., Matsuda, S., Miyake, Y., Yoshimura, A. and Hamaguchi, M. (2000). The JAK-inhibitor, JAB/SOCS-1 selectively inhibits cytokine-induced, but not v-Src induced JAK-STAT activation. *Oncogene* **19**, 4795-4801.

Köster, M., Lykke-Andersen, S., Elnakady, Y. A., Gerth, K., Washausen, P., Hofle, G., Sasse, F., Kjems, J. and Hauser, H. (2003). Ratjadones inhibit nuclear export by blocking CRM1/exportin 1. *Exp. Cell Res.* **286**, 321-331.

Levy, D. E. and Lee, C. K. (2002). What does Stat3 do? *J. Clin. Invest.* **109**, 1143-1148.

Lütticken, C., Wegenka, U. M., Yuan, J., Buschmann, J., Schindler, C., Ziemiecki, A., Harpur, A. G., Wilks, A. F., Yasukawa, K., Taga, T. et al. (1994). Association of transcription factor APRF and protein kinase JAK1 with the interleukin-6 signal transducer gp130. *Science* **263**, 89-92.

Ma, J. and Cao, X. (2006). Regulation of Stat3 nuclear import by importin alpha5 and importin alpha7 via two different functional sequence elements. *Cell. Signal.* **18**, 1117-1126.

Marg, A., Shan, Y., Meyer, T., Meissner, T., Brandenburg, M. and Vinkemeier, U. (2004). Nucleocytoplasmic shuttling by nucleoporins Nup153 and Nup214 and CRM1-dependent nuclear export control the subcellular distribution of latent Stat1. *J. Cell Biol.* **165**, 823-833.

Mingot, J. M., Bohnsack, M. T., Jakle, U. and Gorlich, D. (2004). Exportin 7 defines a novel general nuclear export pathway. *EMBO J.* **23**, 3227-3236.

Nicholson, S. E., De Souza, D., Fabri, L. J., Corbin, J., Willson, T. A., Zhang, J. G., Silva, A., Asimakis, M., Farley, A., Nash, A. D. et al. (2000). Suppressor of cytokine signaling-3 preferentially binds to the SHP-2-binding site on the shared cytokine receptor subunit gp130. *Proc. Natl. Acad. Sci. USA* **97**, 6493-6498.

Niu, G., Wright, K. L., Huang, M., Song, L., Haura, E., Turkson, J., Zhang, S., Wang, T., Sinibaldi, D., Coppola, D. et al. (2002). Constitutive Stat3 activity up-regulates VEGF expression and tumor angiogenesis. *Oncogene* **21**, 2000-2008.

Niu, G., Wright, K. L., Ma, Y., Wright, G. M., Huang, M., Irby, R., Briggs, J., Karras, J., Cress, W. D., Pardoll, D. et al. (2005). Role of Stat3 in regulating p53 expression and function. *Mol. Cell. Biol.* **25**, 7432-7440.

Olayioye, M. A., Beuvink, I., Horsch, K., Daly, J. M. and Hynes, N. E. (1999). ErbB receptor-induced activation of stat transcription factors is mediated by Src tyrosine kinases. *J. Biol. Chem.* **274**, 17209-17218.

Pranada, A. L., Metz, S., Herrmann, A., Heinrich, P. C. and Muller-Newen, G. (2004). Real time analysis of STAT3 nucleocytoplasmic shuttling. *J. Biol. Chem.* **279**, 15114-15123.

Sachsenmaier, C., Sadowski, H. B. and Cooper, J. A. (1999). STAT activation by the PDGF receptor requires juxtamembrane phosphorylation sites but not Src tyrosine kinase activation. *Oncogene* **18**, 3583-3592.

Schlessinger, K. and Levy, D. E. (2005). Malignant transformation but not normal cell growth depends on signal transducer and activator of transcription 3. *Cancer Res.* **65**, 5828-5834.

Schmitz, J., Weissenbach, M., Haan, S., Heinrich, P. C. and Schaper, F. (2000). SOCS3 exerts its inhibitory function on interleukin-6 signal transduction through the SHP2 recruitment site of gp130. *J. Biol. Chem.* **275**, 12848-12856.

Sefton, B. M., Trowbridge, I. S., Cooper, J. A. and Scolnick, E. M. (1982). The transforming proteins of Rous sarcoma virus, Harvey sarcoma virus and Abelson virus contain tightly bound lipid. *Cell* **31**, 465-474.

Sinibaldi, D., Wharton, W., Turkson, J., Bowman, T., Pledger, W. J. and Jove, R. (2000). Induction of p21WAF1/CIP1 and cyclin D1 expression by the Src oncoprotein in mouse fibroblasts: role of activated STAT3 signaling. *Oncogene* **19**, 5419-5427.

Stahl, N., Boulton, T. G., Farruggella, T., Ip, N. Y., Davis, S., Witthuhn, B. A., Quelle, F. W., Silvennoinen, O., Barbieri, G., Pellegrini, S. et al. (1994). Association and activation of Jak-Tyk kinases by CNTF-LIF-OSM-IL-6 beta receptor components. *Science* **263**, 92-95.

Swameye, I., Muller, T. G., Timmer, J., Sandra, O. and Klingmuller, U. (2003). Identification of nucleocytoplasmic cycling as a remote sensor in cellular signaling by databased modeling. *Proc. Natl. Acad. Sci. USA* **100**, 1028-1033.

ten Hoeve, J., de Jesus Ibarra-Sanchez, M., Fu, Y., Zhu, W., Tremblay, M., David,

M. and Shuai, K. (2002). Identification of a nuclear Stat1 protein tyrosine phosphatase. *Mol. Cell. Biol.* **22**, 5662-5668.

Wang, T., Niu, G., Kortylewski, M., Burdelya, L., Shain, K., Zhang, S., Bhattacharya, R., Gabrilovich, D., Heller, R., Coppola, D. et al. (2004). Regulation of the innate and adaptive immune responses by Stat-3 signaling in tumor cells. *Nat. Med.* **10**, 48-54.

Wang, Y. Z., Wharton, W., Garcia, R., Kraker, A., Jove, R. and Pledger, W. J. (2000). Activation of Stat3 preassembled with platelet-derived growth factor beta receptors requires Src kinase activity. *Oncogene* **19**, 2075-2085.

Yahata, Y., Shirakata, Y., Tokumaru, S., Yamasaki, K., Sayama, K., Hanakawa, Y., Detmar, M. and Hashimoto, K. (2003). Nuclear translocation of phosphorylated STAT3 is essential for vascular endothelial growth factor-induced human dermal microvascular endothelial cell migration and tube formation. *J. Biol. Chem.* **278**, 40026-40031.

Yu, C. L., Meyer, D. J., Campbell, G. S., Larner, A. C., Carter-Su, C., Schwartz, J. and Jove, R. (1995). Enhanced DNA-binding activity of a Stat3-related protein in cells transformed by the Src oncoprotein. *Science* **269**, 81-83.

Yu, H. and Jove, R. (2004). The STATs of cancer – new molecular targets come of age. *Nat. Rev. Cancer* **4**, 97-105.

Zeng, R., Aoki, Y., Yoshida, M., Arai, K. and Watanabe, S. (2002). Stat5B shuttles between cytoplasm and nucleus in a cytokine-dependent and -independent manner. *J. Immunol.* **168**, 4567-4575.

Zhang, T., Kee, W. H., Seow, K. T., Fung, W. and Cao, X. (2000a). The coiled-coil domain of Stat3 is essential for its SH2 domain-mediated receptor binding and subsequent activation induced by epidermal growth factor and interleukin-6. *Mol. Cell. Biol.* **20**, 7132-7139.

Zhang, Y., Turkson, J., Carter-Su, C., Smithgall, T., Levitzki, A., Kraker, A., Krolewski, J. J., Medveczky, P. and Jove, R. (2000b). Activation of Stat3 in v-Src-transformed fibroblasts requires cooperation of Jak1 kinase activity. *J. Biol. Chem.* **275**, 24935-24944.